Identification of the Sources of Transient Disturbances

N. R. Watson and A. Farzanehrafat

***Abstract*-- This paper presents a newly developed three-phase transient state estimator based on the equations developed using numerical integrator substitution method (i.e. using Dommel's method of substituting the Trapezoidal rule into the integral equations representing components to form a difference equation). This is faster than the previous state variable formulation. This paper gives an overview of the component models used, and shows how the measurement matrix is built up using measurements and knowledge of the electrical network (encapsulated in these component models). The IEEE 14 busbar test system is used to illustrate the use of the transient state estimator.**

***Keywords*: Transients, State Estimation, Faults**

I. Introduction

TRANSIENT analysis involves modelling the electrical network and disturbance to determine the transient that will result. Transient studies (using programs such as EMTDC, EMTP, ATP,…etc) are used for planning studies to ensure adequate performance as well as diagnostically to investigate and understand events after they have been experienced. This paper however presents a transient state estimator (TSE) which is the reverse of the traditional transient analysis algorithm. The transient state estimator uses recorded transient information and knowledge of the electrical network to identify the type of event and location of the source of the disturbance and is an extension to the well-known fundamental-frequency state estimation used in control rooms. Transient state estimation is in its infancy however, but it holds great promises, particularly with the Smart Grids initiative being promoted worldwide. The major stumbling-block with algorithms such as transient state estimation has been the need of sufficient high quality data which has been a disincentive to developing such algorithm. The need to modernize the electrical grid to enable it to meet the needs of the future is well accepted. This has led to the Smart Grid concept as a pathway of increasing the smartness of the electrical grid so as to meet the demands of the future. Part of this involves two-way communication infrastructure which will make a large amount of data available in the future. This entwining of the electrical network with a communication system promises abundant data in the future for such algorithms to use.

An earlier contribution demonstrated for the first time a transient state estimator based on a state variable formulation [1]-[3]. This paper presents a newly developed three-phase transient state estimator based on the equations developed using numerical integrator substitution (NIS) method (i.e. using Dommel's method of substituting the Trapezoidal rule into the integral equations representing components to form a difference equation [4]). This is faster than the previous formulation and was first demonstrated on a simple single-phase system [5]. This paper details the component models used and shows how the measurement matrix is built up using measurements and knowledge of the electrical network encapsulated in these component models. This is followed by an illustrative example (using the IEEE 14 busbar test system) and final conclusions and future work are discussed.

II. Transient State Estimation

Power Quality State Estimation (PQSE) is a class of state estimation techniques of which TSE is one particular example. Despite the different formulations and quantities they use, the common feature is that they are applying state estimation techniques to power quality problems. Harmonic State Estimation (HSE) and identification of harmonic sources, Transient State Estimation (TSE) and Voltage Dip/Sag State Estimation (VDSE), are all types of PQSE.

The general form of the state estimation problem can be expressed as [6]:

$$\underline{z} = \left[H \right] \underline{x} + \underline{\varepsilon} \tag{1}$$

where z is a (m×1) vector of measured quantities and x is a (n×1) vector of state variables (unknown quantities) for which the equation must be solved. H is a (m×n) measurement function relating the known quantities to state variables and $\underline{\varepsilon}$ is the vector of measurement errors.

Equation (1) is known as the measurement equation and links the measured quantities ($\underline{z}$) to the state variables ($\underline{x}$). For TSE, nodal voltages and branch and load currents are measured quantities and the state variables are nodal voltages.

A. Dynamic Model

To build a measurement equation for TSE a dynamic model representing the system is needed. An earlier contribution

N. R. Watson is with the University of Canterbury, Private Bag 4800, Christchurch, New Zealand (e-mail: neville.watson@canterbury.ac.nz).

A. Farzanehrafat is with the University of Canterbury, Christchurch, New Zealand.

Paper submitted to the International Conference on Power Systems Transients (IPST2013) in Vancouver, Canada July 18-20, 2013.

used a state variable formulation and inductor currents and capacitor voltages as state variables. This work uses the Numerical Integrator Substitution (NIS) method Dommel proposed. The state variables are the node voltages (three nodes per busbar as a three-phase representation). The differential equations are changed to difference equations for each component and a system model developed by using nodal solution. i.e.

$$[G]\underline{v}(t) = \underline{i_s}(t) - \underline{I}_{History}(t) \quad (1)$$

where [*G*] is the conductance matrix, *v(t)* is the vector of nodal voltages, $\underline{i_s}(t)$ is the vector of external current sources and $\underline{I}_{History}(t)$ is the vector current sources representing past history terms. Rather than using for the inductor history term:

$$I_{History}(t) = i(t-\Delta t) + \frac{\Delta t}{2L}\left(v_k(t-\Delta t) - v_m(t-\Delta t)\right) \quad (2)$$

where *L* is the inductance of the inductor connected between nodes *k* & *m*. An alternative form is used, i.e.:

$$I_{History}(t) = 2*i(t-\Delta t) - I_{History}(t-\Delta t) \quad (3)$$

Although (2) and (3) are mathematically equivalent, (3) is slightly more efficient. Moreover, the measurements used in the test system are predominantly current measurements.

B. Component Models

The models developed for electromagnetic transient simulation can, with refinements, be directly used in TSE algorithm [7]-[12]. This section gives a brief sketch of two basic models. The nodal equation for a single-phase nominal π-model transmission line is:

$$\begin{bmatrix} G_{RL}+G_C & -G_{RL} \\ -G_{RL} & G_{RL}+G_C \end{bmatrix} \cdot \begin{bmatrix} V_s(t) \\ V_r(t) \end{bmatrix} = \begin{bmatrix} i_{sr}(t) \\ i_{rs}(t) \end{bmatrix} - \begin{bmatrix} I_{Csh}(t-\Delta t) + I_{RLh}(t-\Delta t) \\ I_{Crh}(t-\Delta t) - I_{RLh}(t-\Delta t) \end{bmatrix} \quad (4)$$

Where $I_{Csh}(t-\Delta t)$ & $I_{Crh}(t-\Delta t)$ are the history terms for the shunt capacitance (sending and receiving end respectively). $I_{RLh}(t-\Delta t)$ is the history term for the series impedance and G_{RL} is its conductance. $i_{sr}(t)$ and $i_{rs}(t)$ are the terminal currents in the line at the sending and receiving ends, respectively.

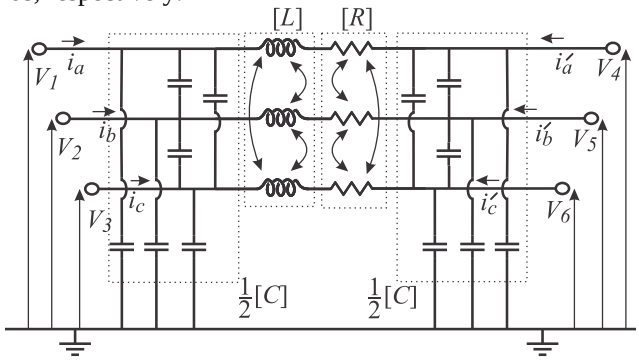

Fig. 1. Three-phase nominal π-model of transmission line.

The extension to a three-phase transmission line model (shown in Fig. 1), uses a matrix format for the lumped line parameters to represent the self & mutual coupling between phases. Therefore, the only difference is that conductance scalar parameters in (4) must be replaced by the appropriate 3×3 matrices. If symmetrical component data is available, this can be accommodated. Considering a the impedance matrix:

$$\boldsymbol{Z} = \begin{bmatrix} Z_{Self} & Z_{Mutual} & Z_{Mutual} \\ Z_{Mutual} & Z_{Self} & Z_{Mutual} \\ Z_{Mutual} & Z_{Mutual} & Z_{Self} \end{bmatrix}$$

Then $Z_{Self} = \frac{2Z^{+Seq} + Z^{0Seq}}{3}$ and $Z_{Mutual} = \frac{Z^{0Seq} - Z^{+Seq}}{3}$

Hence the matrix equation for the nominal π–model is:

$$\begin{bmatrix} [\boldsymbol{G_{RL}}]+[\boldsymbol{G_C}] & -[\boldsymbol{G_{RL}}] \\ -[\boldsymbol{G_{RL}}] & [\boldsymbol{G_{RL}}]+[\boldsymbol{G_C}] \end{bmatrix} \times \begin{bmatrix} \boldsymbol{V_1} \\ \boldsymbol{V_2} \\ \boldsymbol{V_3} \\ \boldsymbol{V_4} \\ \boldsymbol{V_5} \\ \boldsymbol{V_6} \end{bmatrix} = \begin{bmatrix} \boldsymbol{i_a(t)} \\ \boldsymbol{i_b(t)} \\ \boldsymbol{i_c(t)} \\ \boldsymbol{i'_a(t)} \\ \boldsymbol{i'_b(t)} \\ \boldsymbol{i'_c(t)} \end{bmatrix} - \begin{bmatrix} \boldsymbol{I_{a\_History}} \\ \boldsymbol{I_{b\_History}} \\ \boldsymbol{I_{c\_History}} \\ \boldsymbol{I_{a'\_History}} \\ \boldsymbol{I_{b'\_History}} \\ \boldsymbol{I_{c'\_History}} \end{bmatrix} \quad (5)$$

Three-phase transformers are modelled by three ideal single-phase transformers represented by a mutual inductance coupling between windings (6). Hence the fundamental equation is:

$$\frac{d}{dt}\begin{bmatrix} i_1(t) \\ i_2(t) \end{bmatrix} = \frac{1}{L}\begin{bmatrix} 1 & -a \\ -a & a^2 \end{bmatrix} \cdot \begin{bmatrix} v_1(t) \\ v_2(t) \end{bmatrix} \quad (6)$$

where $L = L_1 + a^2 L_2$, is leakage inductance between primary and secondary windings as measured from primary winding. Applying Trapezoidal rule to (6) and rearranging equation to the form of (1) yields:

$$\frac{\Delta t}{2L}\begin{bmatrix} 1 & -a \\ -a & a^2 \end{bmatrix} \cdot \begin{bmatrix} v_1(t) \\ v_2(t) \end{bmatrix} = \begin{bmatrix} i_1(t) \\ i_2(t) \end{bmatrix} - \begin{bmatrix} I_{1History}(t-\Delta t) \\ I_{2History}(t-\Delta t) \end{bmatrix} \quad (7)$$

where the history terms can be calculated as:

$$\begin{bmatrix} I_{1History}(t-\Delta t) \\ I_{2History}(t-\Delta t) \end{bmatrix} = \begin{bmatrix} i_1(t-\Delta t) \\ i_2(t-\Delta t) \end{bmatrix} + \frac{\Delta t}{2L}\begin{bmatrix} 1 & -a \\ -a & a^2 \end{bmatrix} \cdot \begin{bmatrix} v_1(t-\Delta t) \\ v_2(t-\Delta t) \end{bmatrix}$$

This can be extended to a three-phase transformer by considering the transformer configuration. Connection matrices are used to derive the nodal equation based on coil configuration (e.g. delta/star, star/star,… etc). Regardless of the transformer configuration the three-phase transformer can be represented by the matrix equation:

$$\boldsymbol{G_{winding}}\boldsymbol{v_{winding}}(\boldsymbol{t}) = \boldsymbol{i_{winding}}(\boldsymbol{t}) - \boldsymbol{I_{History_{winding}}}(\boldsymbol{t}-\Delta\boldsymbol{t}) \quad (8)$$

The transformer configuration is accommodated by considering the relationship between the winding currents and voltages, and the nodal currents and voltages. Consider for example a three-phase delta/star-g transformer. The relationship between node quantities and winding quantities, with all nodal voltages being with respect to the reference earth, can be defined as follows:

$$\boldsymbol{v_{winding}} = \boldsymbol{C} \cdot \boldsymbol{V_{Node}} \quad (9)$$

$$\boldsymbol{i_{winding}} = \boldsymbol{C^T} \cdot \boldsymbol{I_{Node}} \quad (10)$$

where ***C***, connection matrix, for a delta/star-g configuration is:

$$\boldsymbol{C} = \begin{bmatrix} 1 & -1 & 0 & 0 & 0 & 0 \\ 0 & 1 & -1 & 0 & 0 & 0 \\ -1 & 0 & 1 & 0 & 0 & 0 \\ 0 & 0 & 0 & 1 & 0 & 0 \\ 0 & 0 & 0 & 0 & 1 & 0 \\ 0 & 0 & 0 & 0 & 0 & 1 \end{bmatrix} \quad (11)$$

Substituting the winding parameters with nodal parameters in (8) yields:

$$G_{winding} CV_{Node} = \left(C^T\right)^{-1} \left(I_{Node}(t) - I_{Hist_{Node}}(t - \Delta t)\right) \quad (12)$$

Multiplying both sides by $\boldsymbol{C^T}$ gives:

$$C^T G_{winding} CV_{Node} = I_{Node}(t) - I_{History_{Node}}(t - \Delta t) \quad (13)$$

The term $\boldsymbol{C^T.G_{winding}.C}$ is the nodal conductance matrix for a three-phase transformer and it is added to the appropriate entries of the system nodal conductance matrix ([G]).

C. Formation of Measurement Equation

Each measurement point results in one equation being added to the measurement equation by adding the appropriate information from the dynamic model into $\boldsymbol{H}$, to form the TSE measurement equation. Table I indicates how the $\boldsymbol{H}$ matrix entries are built from elements of the $\boldsymbol{G}$ matrix (for current measurements) and ones & zeros (for voltage measurements). For example, when a node voltage is measured the corresponding row in the $\boldsymbol{H}$ matrix will be zero except at the position corresponding to the node that was. A branch current measurement will add a row to $\boldsymbol{H}$ consisting entirely of zeros except at the locations associated with the sending and receiving end nodes, which will contain the appropriate conductance entries from the $\boldsymbol{H}$ matrix.

TABLE I
MEASUREMENT EQUATION CONSTRUCTION

Measurement Type	Measurement Vector Entry (z)	Measurement Matrix $\boldsymbol{H}$
Phase Voltage	$v_k(t)$	[0...0,1,0...0]
Branch Voltage	$v_k(t) - v_m(t)$	[0..0,1,0..0,-1, 0…0]
Branch Current	$i_{km}(t)$-$I_{History}(t)$	[0...0,G_{eff},0...0 , -G_{eff} , 0...0]

D. Solution of Measurement Equation

The solution methods available depend on the rank of the H matrix and whether the system is under-determined or over-determined, or just observable. Singular Value Decomposition (SVD) is the solution method of choice due to; its ability to solve under-determined systems and give observability information, as well as its robustness [6][13]. SVD factors the measurement matrix, i.e.:

$$H = [U][W][V]^T \quad (14)$$

where U (m×n) and V^T (n×n) are orthogonal matrices and W (n×n) is a diagonal matrix with entries of singular values of H. This factorization is employed to compute a pseudo-inverse of the measurement matrix H, and use this to calculate the state variables:

$$\underline{x} = [V][W]^{-1}[U]^T z \quad (15)$$

III. APPLICATION OF TSE

A. Test System

The 60 Hz IEEE 14 busbar test system [14] is used to demonstrate the capability of TSE. The measurement points are illustrated in Fig. 2. With this measurement placement the system is unobservable as there are insufficient measurements to determine all state variables. Busbar 1 is unobservable. A line-to-ground fault is applied at busbar 13. A line-to-ground fault is simulated as general it is a more testing case for a three-phase algorithm (testing the self and mutual impedance terms). The IEEE 14 busbar system was simulated in PSCAD/EMTDC and the results taken as actual measurements. The power system components have been modelled according to the modelling guidelines for voltage dip studies (Table VI of [11] & [8]-[10]).

The PSCAD/EMTDC results at the measurement locations are then fed into the TSE algorithm and the TSE estimates the voltages and currents at the unmonitored locations. The estimates are inspected and compared to the actual.

A 50 μs time-step was used for the PSCAD/EMTDC simulation and hence the component models used for developing the TSE also used a 50 μs time-step.

B. Simulation Results

Figs. 3-7 show representative samples of the results from application of the TSE algorithm. As can be seen there is a very good match between estimated and actual for all busbars except busbar 1 which is unobservable. From the voltage depression at the different busbars it is easy to identify busbar 13 as the location of the fault. Moreover the singular values identify the unobservable busbar, however, ever from the solution the unobservable busbar is obvious as SVD gives the minimum norm solution (hence zero if unobservable).

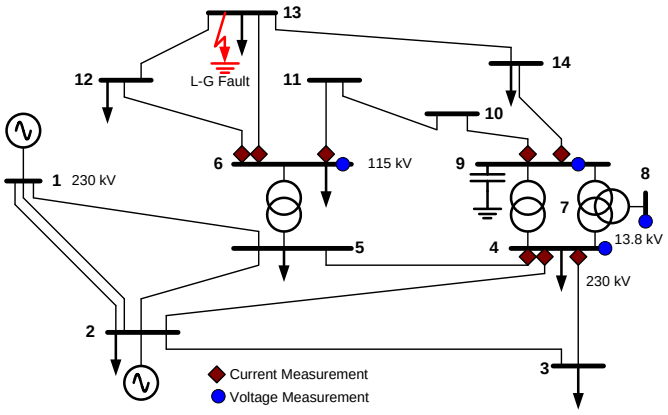

Fig. 2. IEEE 14 busbar test system.

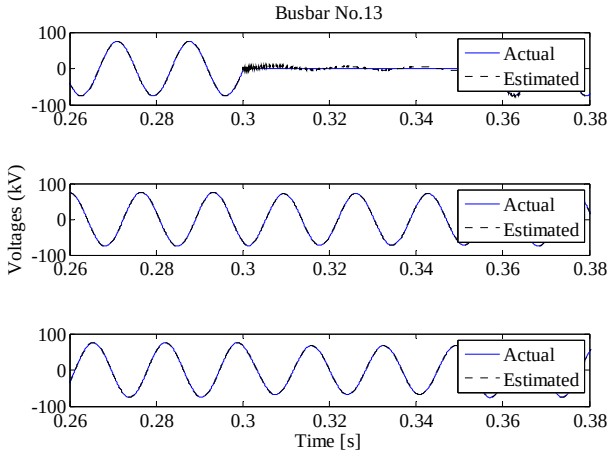

Fig. 3. Estimated and actual voltage at busbar 13.

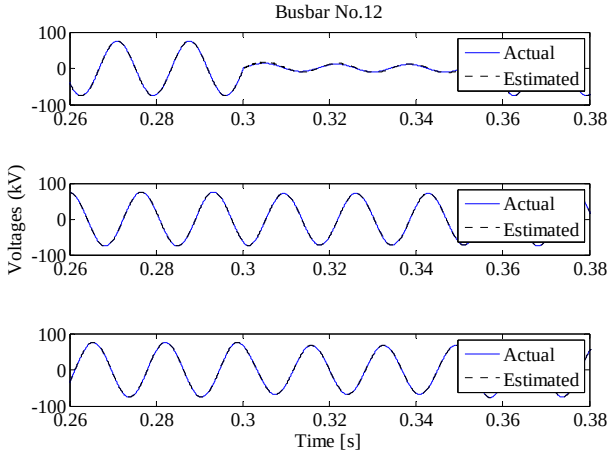

Fig. 4. Estimated and actual voltage at busbar 12.

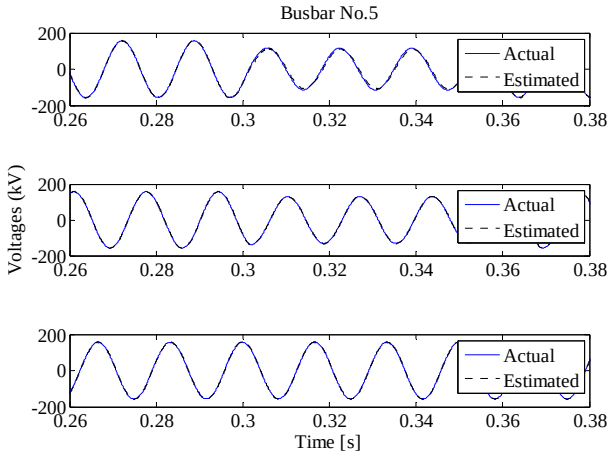

Fig. 5. Estimated and actual voltage at busbar 5.

Close inspection of difference between estimated and actual at the fault location (displayed in Fig. 8) shows some small numerical oscillations. To understand these oscillations further the measurements are cut back to voltage measurements at busbar 6 and line currents in line 6 to 13 only, for this IEEE 14 busbar system. Figs. 9 & 10 display the comparison and error for busbar 13 in this case. An oscillation is evident around the true value, although of small magnitude and will not affect the ability to identify the source of the transient disturbance. As TSE uses the Trapezoidal rule to discretize the differential equations to form difference equations the same numerical issues already encountered with simulation with abrupt changes are to be expected.

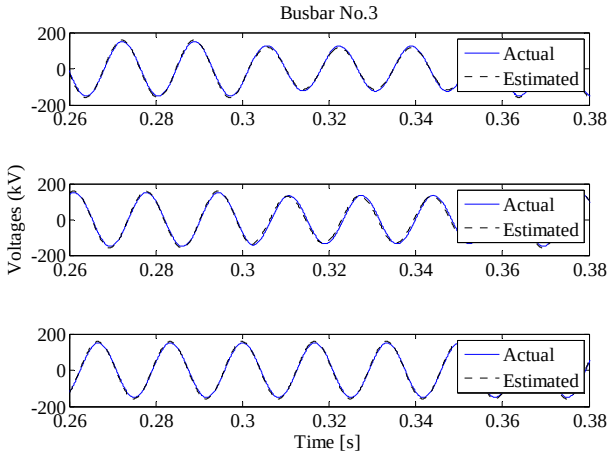

Fig. 6. Estimated and actual voltage at busbar 3.

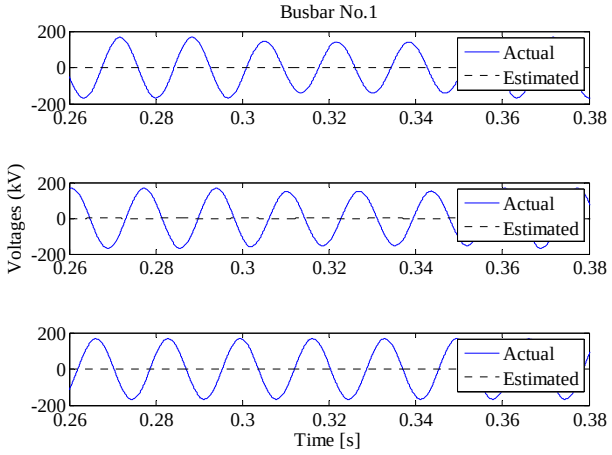

Fig. 7. Estimated and actual voltage at busbar 1.

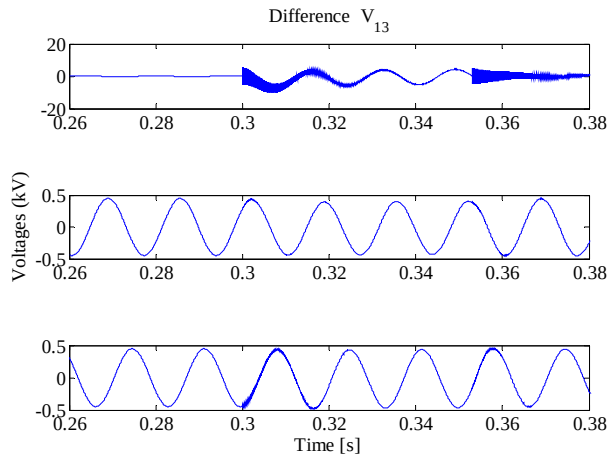

Fig. 8. Error in busbar 13 voltage estimate.

To verify that this is due to the well documented numerical oscillation that occurs with Trapezoidal rule a rectangular integrator (that is the backward Euler method) was substituted in instead of the Trapezoidal rule. The same IEEE 14 busbar system is used. Figs. 11 & 12 display the comparison and error, respectively, for busbar 13 using this new discretization for the TSE. Figs. 11 & 12 do not show this oscillation and give extremely good results. There is no tendency for numerical oscillations as would be expected for the backward Euler method.

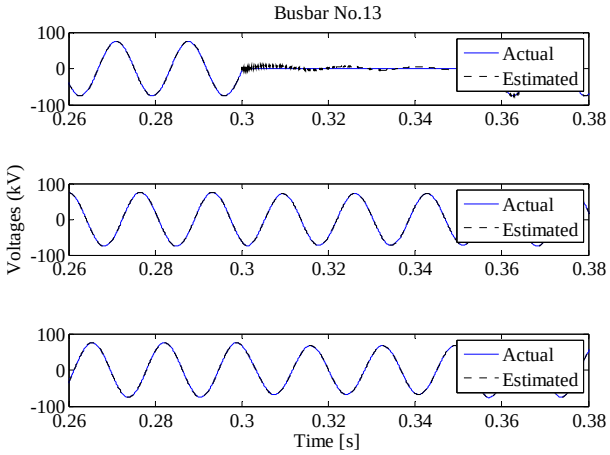

Fig. 9. Estimated and actual voltage at busbar 13 (Trapezoidal Integrator).

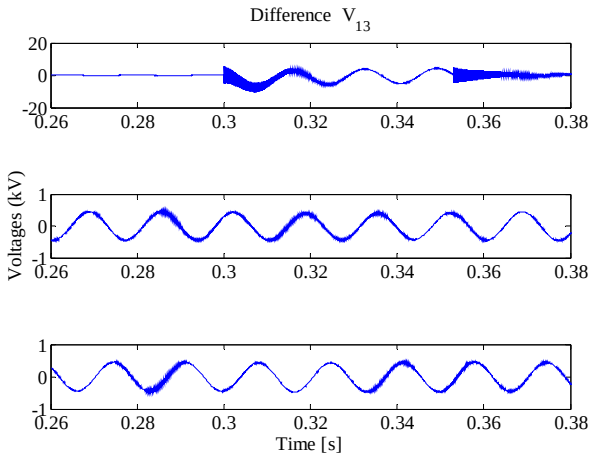

Fig. 10. Error in busbar 13 voltage estimate (Trapezoidal Integrator).

Another more robust and accurate technique is the root-matching method [10]. This method is extremely robust and accurate with no tendency for numerical oscillations. Applying the root-matching technique to form a new TSE gives the excellent results shown in Figs. 13 & 14. This test involved applying the root-matching method to the transmission line model as a line current measurement was used. Although the root-matching technique it is already used for the Continuous System Model Functions (CSMF) toolbox in PSCAD/EMTDC it is not used for the other electrical components. For a general TSE further working is needed to adapt the other component models to use the root-matching approach.

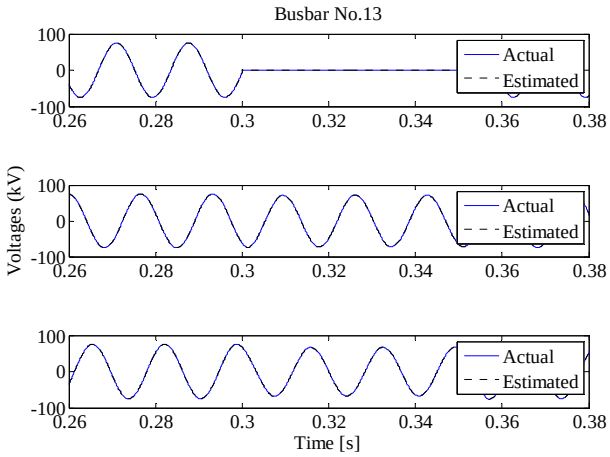

Fig. 11. Estimated and actual voltage at busbar 13 (rectangular integrator).

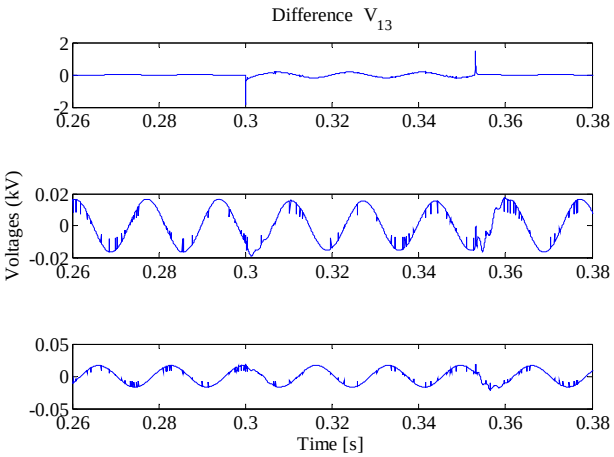

Fig. 12. Error in busbar 13 voltage estimate (rectangular integrator).

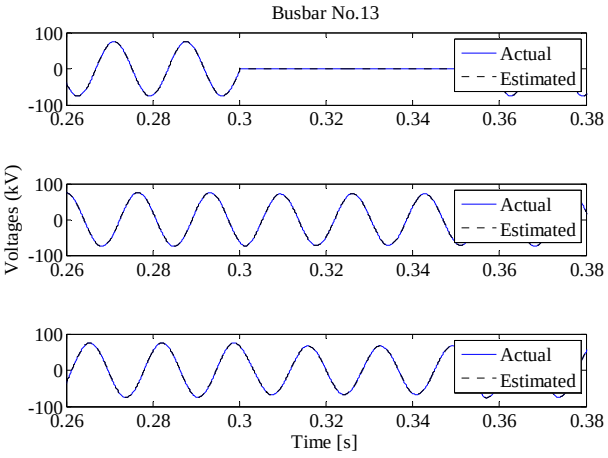

Fig. 13. Estimated and actual voltage at busbar 13 (root-matching).

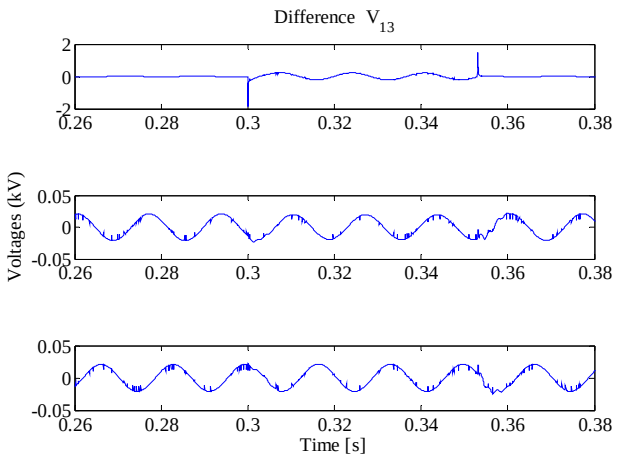

Fig. 14. Error in busbar 13 voltage estimate (root-matching).

IV. Conclusions

The concept of transient state estimation using numerical integrator substitution formulation has been presented. The basic three-phase component models have been given and illustrative results using the IEEE 14 busbar test system presented. The results demonstrated that the technique is well suited for identifying the sources of transient disturbances. The TSE method based on NIS works very well but is subject to the same limitations already encountered in electromagnetic transient simulation.

Oscillations around the true values were observed on some of the estimated voltage waveforms and these were verified to be due to numerical noise inherent in the Trapezoidal rule at sharp discontinuities. In order to verify this two new TSE were formed by reformulated using backward Euler integrator and root-matching technique and the performance of these new TSEs were verified. This is the first time a TSE using backward Euler integrator and root-matching technique have been demonstrated. Root-matching is particularly promising due to its characteristics and even lower computation (as the exponential term can be calculated prior to time-stepping) than the traditional NIS methods.

It has been demonstrated that TSE is a powerful tool in identifying the source location of transient disturbances. One of the main barriers for practical implementation of TSE is the present lack of suitable measurement data (hence the need to use simulation data in this paper). However, as Smart Grids evolves the number of measurements is not likely to be the barrier it once was due to the massive amount of data that is becoming available.

Since TSE is in its infancy compared to electromagnetic transient simulation there are many avenues open for improvement. More work is needed to improve the models further. In particular incorporating travelling-wave transmission line model is important to increase the TSE's applicability to transmission systems. Early performance tests with measurement noise have been encouraging and more work on this (and bad-data detection and removal) are needed. Also testing with high impedance faults is required.

The use of root-matching technique to develop a new TSE has been demonstrated and this needs developing further. However, if the Trapezoidal integrator is retained chatter removal methods need to be incorporated to overcome numerical noise. In the future incorporation of load current measurements without the need to know the load composition could be achieved to add more information (as this has already been accomplished for harmonic state estimation).

V. Acknowledgment

The authors gratefully acknowledge the help of Associate Professor Sarath Perera (University of Wollongong, Australia), for hosting Mr. Farzanehrafat, to enable him to escape the considerable upheavals due to the Christchurch earthquakes and continue his research work.

VI. References

[1] K. K. C. Yu and N. R. Watson, "Identification of Fault Locations using Transient State Estimation," in *International Power System Transient (IPST2005)*, Montreal (Canada), 2005.

[2] K. K. C. Yu and N. R. Watson, "An approximate method for transient state estimation," *IEEE Trans. Power Delivery*, vol. 22, pp. 1680-1687, July 2007.

[3] N. R. Watson and K. K. C. Yu, "Transient State Estimation," in *13th Int. Conf. on Harmonics and Quality of Power(ICHQP)*, 2008, pp. 1-6.

[4] H. W. Dommel, "Digital Computer Solution of Electromagnetic Transients in Single- and Multiphase Networks," *IEEE Trans. Power Apparatus and Systems*, vol. PAS-88, pp. 388-399, 1969.

[5] N. R. Watson, "Power quality state estimation," *European Transactions on Electrical Power*, vol. 20, pp. 19-33, Jan 2010.

[6] J. Arrillaga, N.R. Watson & S. Chen, *Power system quality assessment*, Chichester (UK), John Wiley & Sons, 2000, p. 300.

[7] H. W. Dommel, "Digital Computer Solution of Electromagnetic Transients in Single- and Multiphase Networks," *IEEE Trans. on Power Apparatus and Systems*, vol. PAS-88, pp. 388-399, 1969.

[8] H. W. Dommel, *Electromagnetic Transients Program Reference Manual (EMTP Theory Book)*. Portland: Bonneville Power Administration, 1986.

[9] IEEE Working Group 15.08.09, *Modeling and Analysis of System Transients using Digital Programs*, Tutorial TP-133-0, Piscataway (USA), IEEE/PES, 1999.

[10] N. R. Watson and J. Arrillaga, *Power systems electromagnetic transients simulation.* London: Institution of Electrical Engineers, 2002.

[11] CIGRE Task Force C4.102: *Voltage Dip Evaluation and Prediction Tools*, 2009.

[12] J. A. Martinez-Velasco, *Power System Transients*, Boca Raton, CRC Press, 2010.

[13] W. H. Press, *Numerical recipes: the art of scientific computing*, 3rd ed. Cambridge, UK ; New York: Cambridge University Press, 2007.

[14] R. Abu-Hashim, R. Burch, G Chang, M. Grady, E. Gunther, M. Halpin, C. Harziadonin, Y. Liu, M. Marz, T. Ortmeyer, V. Rajagopalan, S. Ranade, P. Ribeiro, T. Sim, T. W. Xu, "Test systems for harmonics modeling and simulation", *IEEE Trans. on Power Delivery*, vol. 14, no. 2, pp. 579- 587, April 1999.